ELSEVIER

Journal of Chromatography B, 664 (1995) 17–31

JOURNAL OF CHROMATOGRAPHY B: BIOMEDICAL APPLICATIONS

Preparative-scale amino acid separation by thermal parametric pumping on an ion-exchange resin

Gabor Simon[a,b], Laszlo Hanak[b], Georges Grevillot[a,*], Tibor Szanya[b], Gyula Marton[b]

[a]*Laboratoire des Sciences du Genie Chimique, CNRS–ENSIC, B.P. 451, 54001 Nancy, France*
[b]*Department of Chemical Engineering, University of Veszprem, Veszprem, Hungary*

Abstract

Thermal parametric pumping was experimentally investigated for the concentration and separation of amino acids. Previous theories of parametric pumping were improved by taking into account dissociation equilibria in the liquid phase. Experiments were carried out with a mixture of glutamic acid, aspartic acid, serine and threonine in a highly acidic solution (HCl). A multi-component equilibrium model was mainly used to simulate the experimental results and to investigate the effect of chloride concentration over a wide range. It is shown that it is always possible to concentrate the amino acids and to separate some of them under certain conditions.

1. Introduction

Every year a great amount of waste, which contains proteins, is produced. After acidic, basic or enzymatic hydrolysis, these materials can be used as a natural source of amino acids. Generally, the individual amino acids are isolated by multi-step adsorption and ion-exchange methods. The objectives of this study concern the industrial importance of ion-exchange processes as a means of recovering, separating and purifying amino acids and amino acid mixtures. Amino acids have acquired a very important role in industry and are among the largest volume products of biotechnology.

Ion exchange is widely used in various stages of the processes. Ion-exchange resins exhibit a high capacity for amino acids and the selectivity can be changed by adjusting the solution pH, thus exploiting the amphoteric nature of amino acids. Recovery of amino acids from dilute solution using a cation-exchange resin can thus be carried out in a cyclic process consisting of a low-pH adsorption period followed by a high-pH regeneration, or desorption, period during which the amino acid is recovered in concentrated form.

In order to avoid chemicals such as acids, salts and buffers for chemical and environmental reasons, other sources of energy for the separations could be investigated. In this area, thermal parametric pumping is a technique which uses thermal energy at low potential. It is based on the periodic movement of a fluid phase over a solid adsorbent bed and a coupled energy input into the system to effect the separation. The most common form of parametric pumping is one in which a packed bed of adsorbent, under-

* Corresponding author.

0378-4347/95/$09.50
SSDI 0378-4347(94)00428-5

going a cycling temperature change, is subjected to a synchronous, alternating, axial flow. The variation of adsorption isotherms with temperature (or other thermodynamic parameters such as ionic strength or pH) and the synchronized relative motion of the fluid over the fixed phase make possible the enrichment of a given component at one end of the column and its depletion at the other end.

The analogy with distillation has been described by Grevillot and Tondeur [1,2]. At total reflux, the vapour from the top of the column is condensed and returns as liquid into the column. In parametric pumping, the upward flow during the hot half-cycle is analogous to the vapour in distillation and the downward flow during the cold half-cycle is analogous to the liquid in distillation. The adsorption isotherms at the two temperatures play the role of the liquid–vapour equilibrium curve. As in total reflux distillation, in batch parametric pumping there is no feed and no withdrawals: all of the liquid collected in the top (bottom) reservoir during the hot (cold) half-cycle is returned to the column during the cold (hot) half-cycle. Parametric pumping can be also operated at partial reflux in several ways (continuous, semi-continuous, intermediate feed position, etc.). The temperature change can be applied to the column itself (direct mode) or by the fluid itself (recuperative mode).

Wilhelm et al. [3] first described the separation of an aqueous NaCl solution into two fractions, one enriched and the other depleted in NaCl. The potential of the technique was demonstrated by Wilhelm and Sweed [4] when they obtained a separation factor of 10^5 in a toluene–*n*-heptane–silica gel system under total reflux conditions. This high separation capability provides an incentive for the development of mathematical models that could predict separations.

Pigford et al. [5] developed an important and simple equilibrium theory and derived mathematical expressions for the performance of the batch parametric pump [4]. Two primary assumptions of the theory were instantaneous local equilibrium throughout the adsorption column with linear equilibria and absence of axial dispersion. Later, Aris [6] showed that the theory of Pigford et al. [5] is a special case of a more general theory and derived the general theory.

By extending the equilibrium theory, Chen and co-workers [7–9] derived mathematical expressions for the performance of batch, continuous and semi-continuous parametric pumps. They showed that under certain conditions the batch pump and the continuous and semi-continuous pumps with feed at the enriched end have the capacity for complete removal of solute from one product stream and, at the same time, give an arbitrarily large enrichment of solute in the other product stream.

Sabadell and Sweed [10] carried out separations using a recuperative-mode pH pump in which pH control was maintained by acid addition to one of the end reservoirs.

Several reviews [11–14] also show the interest in using parametric pumping for different kinds of separations. In this work, two new aspects of parametric pumping were investigated: first, application to amino acid separations, and second, the effect of dissociation reactions in solution.

2. Principles of parametric pumping

The principles of parametric pumping can be easily understood from Fig. 1, where the steps of the cyclic operation are illustrated with the help of a McCabe–Thiele type diagram.The hot and cold isotherms are shown and it is clear that the uptake is greater at a cold temperature than at a hot temperature.

The operation starts with a first step to obtain the initial conditions:

Step 1. The column is equilibrated at a cold temperature with the solution to be separated and the bottom reservoir is filled with the same solution (point A on the isotherms).

After this, a cycle consists of the following steps:

Step 2. The column is heated to the hot temperature (point B on the isotherms).

Step 3. The solution from the bottom reservoir is pumped to the top reservoir through the

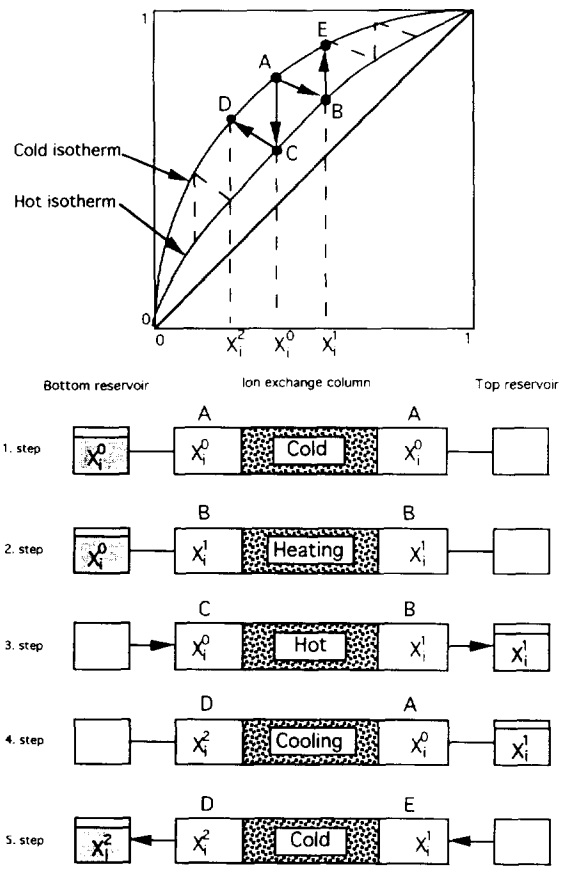

Fig. 1. Principles of parametric pumping.

column at a hot temperature (points C and B on the isotherms).

Step 4. The column is cooled to the cold temperature (points D and A on the isotherms).

Step 5. The solution from top reservoir is pumped to the bottom reservoir through the column at a cold temperature (points E and D on the isotherms).

Steps 2–5 are repeated until the desired cycle number is reached.

It can be also seen on Fig. 1 that the ionic fraction of component i increases in the top reservoir and decreases in the bottom reservoir. This model gives a good qualitative understanding of how the separation develops, but it is usually insufficient to represent results quantitatively.

3. Theory

Let us consider a thermal direct-mode batch parametric pump, which is a cyclic operation device with a hot upwards half-cycle and a cold downwards half-cycle. We assume instantaneous local equilibrium, plug flow, instantaneous heating and cooling and flow reversal in phase with temperature change.

In our case the system contains from two to four amino acid cations [aspartic acid (Asp), glutamic acid (Glu), serine (Ser), threonine (Thr) and in some cases proline (Pro)] and hydrogen ions; co-ions are amino acid anions, hydroxyl ion and chloride ion. In addition, the zwitterionic forms of the amino acids are also present.

As shown by Carta and co-workers [15,16], it is convenient to write the material balance for the total concentration C_{A_i} of the amino acid i. The local pH and the concentrations of the cationic, anionic and zwitterionic forms can then be calculated from the electroneutrality conditions. An additional material balance is needed for the chloride ion if this is present and variable.

The material balance over a differential volume element of an ion-exchange column is

$$v \cdot \frac{\partial C_{A_i}}{\partial z} + \frac{\partial C_{A_i}}{\partial t} + \frac{1-\varepsilon}{\varepsilon} \cdot \frac{\partial q_{A_i}}{\partial t} = 0 \qquad (1)$$

where C_{A_i} is the concentration of a given amino acid in the fluid phase, q_{A_i} is the amino acid concentration in the solid phase, v is the interstitial velocity and $\varepsilon = 0.35$ is the bed void fraction. To solve this equation it is necessary to have a description of the uptake equilibrium on the resin. The selectivity coefficient for exchange of ion i with ion j at temperature T is

$$S_{i,j}^{T} = \frac{y_i^T x_j^T}{y_j^T x_i^T} \qquad (2)$$

where x_i^T is the ionic fraction of amino acid cation i in solution at temperature T and y_i^T is the ionic fraction of cation i in the resin at temperature T.

Dye et al. [17] expressed the multi-component uptake of amino acids as a function of the ionic fractions of amino acid cations and hydrogen ions as

$$y_{A_i} = \frac{q_{A_i}}{q_0} = \frac{S_i x_{A_i}}{x_H + \sum_i S_i x_{A_i}} \quad (3)$$

where q_0 is the ion-exchange capacity of the resin, S_i is the binary ion-exchange selectivity for cation i relative to hydrogen ion and x_{A_i} and x_H are the liquid-phase ionic fraction of amino acid cation i and hydrogen respectively. This equation includes the electroneutrality condition in the resin.

The ionic fractions x_{A_i} are given by

$$x_{A_i} = \frac{C_{A_i^+}}{C_{H^+} + \sum_k C_{A_k^+}} \quad (4)$$

where $C_{A_i^+}$ is the concentration of amino acid cation i and C_{H^+} is the hydrogen ion concentration. The total concentration of each amino acid, C_{A_i}, is equal to the sum of all its ionic forms and can be calculated from

$$C_{A_i} = C_{A_i^+} + C_{A_i^\pm} + C_{A_i^-} + C_{A_i^{2-}} \quad (5)$$

where for each amino acid:

$$C_{A_i^+} = C_{A_i} \Big/ \left(1 + \frac{K_{1_i}}{C_{H^+}} + \frac{K_{1_i}K_{2_i}}{C_{H^+}^2} + \frac{K_{1_i}K_{2_i}K_{3_i}}{C_{H^+}^3}\right) \quad (6)$$

$$C_{A_i^-} = C_{A_i} \Big/ \left(1 + \frac{C_{H^+}}{K_{2_i}} + \frac{C_{H^+}^2}{K_{1_i}K_{2_i}} + \frac{K_{3_i}}{C_{H^+}}\right) \quad (7)$$

$$C_{A_i^{2-}} = C_{A_i} \Big/ \left(1 + \frac{C_{H^+}}{K_{3_i}} + \frac{C_{H^+}^2}{K_{2_i}K_{3_i}} + \frac{C_{H^+}^3}{K_{1_i}K_{2_i}K_{3_i}}\right) \quad (8)$$

where K_{1i}, K_{2i} and K_{3i} are the dissociation constants of the amino acids. For neutral amino acids (threonine, serine, proline) K_3 and $C_{A^{2-}}$ are zero. The dissociation constants of the amino acids are given in Table 1. Finally, the electroneutrality condition in the liquid phase is expressed by

Table 1
Dissociation constants of amino acids

Amino acid	pK_{1i}	pK_{2i}	pK_{3i}
Asp	1.88	3.65	9.6
Glu	2.19	4.25	9.67
Pro	1.99	10.60	–
Ser	2.21	9.15	–
Thr	2.09	9.10	–

$$\sum_i C_{A_i^+} + C_{H^+} = \sum_i C_{A_i^-} + C_{Cl^-} + \frac{K_w}{C_{H^+}} + 2\sum_i C_{A_i^{2-}} \quad (9)$$

where K_w is the ionic product of water.

The model was solved with a finite difference method. To carry out the numerical computation, the boundary conditions and the initial conditions are assigned. These conditions always change when a new half-cycle is started, so there is no reason to go into detail.

This model was used in the theoretical study of the influence of chloride concentration. For the calculations, connected with the experiments, the model is simplified, because all of the amino acids can be assumed to be positively charged and the total cation concentration equal to the chloride concentration (this is an extreme case of the theory, mentioned before, and leads to the same results with less calculation).

Calculations with a simpler theory (Pigford et al.'s theory, which is based on the assumption of local equilibrium between solid and liquid phase and linear isotherms [5]) were also carried out to predict rapidly the experimental separations and for comparison.

The material balance is expressed by Eq. 1. If the equilibrium relation is linear:

$$q = K^T C \quad (10)$$

where K^T is the distribution coefficient at temperature T. The relationship between S^T and K^T in the linear range is

$$S^T = K^T \cdot \frac{C_0}{q_0} \quad (11)$$

where C_0 is the total cation concentration and q_0 is the ion-exchange capacity of the resin. By solving Eq. 1, the following expression is obtained:

$$\frac{dz}{dt} = u = \frac{v}{\varepsilon + (1-\varepsilon)K^T} \tag{12}$$

where u represents the velocity of a concentration step in the isothermal bed.

The new equilibrium composition due to the temperature change for a Δz part of the column is as follows:

$$A\varepsilon C_h \Delta z + A(1-\varepsilon)q_h \Delta z = A\varepsilon C_c \Delta z + A(1-\varepsilon)q_c \Delta z \tag{13}$$

where A is the cross-sectional area of the column, C_h and C_c are the concentrations in the liquid phase at hot and cold temperatures, respectively, and q_h and q_c are the concentrations in the resin at hot and cold temperatures, respectively. If Eq. 10 is inserted into Eq. 13 and rearranged, one obtains

$$\frac{C_h}{C_c} = \frac{\varepsilon + (1-\varepsilon)K_c}{\varepsilon + (1-\varepsilon)K_h} = \frac{u_h}{u_c} \tag{14}$$

where K_h and K_c are the distribution coefficients at hot and cold temperatures, respectively. Since u_h (the velocity of a concentration step at a hot temperature) is always higher than u_c (the velocity of a concentration step at a cold temperature), after n cycles the concentration in the bottom reservoir can be expressed as follows:

$$C_n = C_0\left[\frac{\varepsilon + (1-\varepsilon)K_h}{\varepsilon + (1-\varepsilon)K_c}\right]^n \tag{15}$$

The situation is different at the top reservoir because except for the first hot flow, at least one concentration step reaches the reservoir. The expression of reservoir concentrations is more complicated, and therefore we use a computer to solve the problem.

4. Experimental

4.1. Materials and methods of analysis

The resin used was Dowex 50W-X8 with 100–200 mesh particle size. Before use the resin was treated by repeated cycles of washing with 1 *M* HCl and 1 *M* NaOH solution to remove impurities. Then it was prepared in the hydrogen form.

The amino acids were obtained from Reanal (Budapest, Hungary) with purity greater than 99%, and needed no further purification. Other chemicals were of analytical-reagent grade.

4.2. Equilibrium data for parametric pumping

To obtain a separation by parametric pumping, it is necessary that the equilibrium data vary with temperature. Since

$$\frac{d\ln K^T}{dT} = \frac{\Delta H}{RT^2} \tag{16}$$

where K^T is the distribution coefficient, T is the absolute temperature, ΔH is the heat of the ion-exchange reaction and R is the universal gas constant, if $\Delta H \neq 0$ then the distribution coefficient varies with temperature and if $\Delta H < 0$ then K^T decreases with increasing temperature.

We measured the distribution coefficients of the amino acids by the elution method [18]. An ion-exchange column in the H^+ form was percolated with 1.0 *M* HCl and a single-component amino acid sample (0.1 *M*) was injected into this eluent stream. In this limited range of concentrations, the equilibrium relation between q and C is linear (Eq. 10). We determined the K^T values from the retention volume of the experimentally obtained chromatographic peaks:

$$V_R = V_c\varepsilon + V_c(1-\varepsilon)K^T + \frac{V_i}{2} \tag{17}$$

where V_R is the retention volume of the chromatographic peak, V_c is the volume of the bed ($V_c = 20$ cm^3) and V_i is the volume of pulse injection ($V_i = 2$ cm^3). To investigate the effect of temperature, two runs were carried out at 288 and 363 K under the same conditions. The distribution coefficients for amino acids are given in Table 2 for these two temperatures (K_c and K_h, respectively). We found that the amino acid uptake in all instances decreases with increasing temperature. Proline's affinity seems to be the greatest at both cold and hot temperatures, and

Table 2
Distribution coefficients in 1.0 *M* HCl

Amino acid	K_c	K_h	K_c/K_h
Asp	2.67	1.93	1.38
Glu	3.24	1.92	1.68
Ser	2.67	2.14	1.25
Thr	2.74	2.34	1.17
Pro	8.34	5.54	1.51

the temperature dependence of the distribution coefficient, represented by the ratio K_c/K_h, is the greatest with glutamic acid. The K_c/K_h values play a very important role in parametric pumping, because the greatest temperature dependence of the equilibrium data means the greatest parametric pumping effect.

By applying Eq. 11, we can calculate the binary ion-exchange selectivity for an amino acid cation relative to hydrogen ion ($q_0 = 2.08$ mol/l dry resin). According to Eq. 11, S^T is directly proportional to K^T. Thus the same statements are true for both variables.

4.3. Results of experiments

A schematic diagram of the experimental apparatus is shown in Fig. 2. A jacketed glass column (50 cm × 1.0 cm I.D.) was filled with the resin and reservoirs were connected to both ends. A constant temperature of the column was maintained by use of thermostated baths, which supplied water at 288 and 363 K. The movement of the solution through the column was accomplished by use of peristaltic pump; the flow-rate was 2 cm^3/min.

Before starting the experiment the column was equilibrated at the cold temperature with the solution intended to be separated. Then a given volume of solution (ΔV) with the same composition was poured into the bottom reservoir and the parametric pumping experiment was started. After the desired number of cycles had elapsed, samples were taken from the mixed reservoirs for analytical purposes. These samples were kept small so that several could be taken during each run without changing the total amount of material in the system. The concentration of amino acids was measured with an amino acid analyser (Aminochrom II, OE-914; Labor-MIM, Budapest, Hungary). The analyser operates on the basis of the colour reaction amino acids with ninhydrin solution.

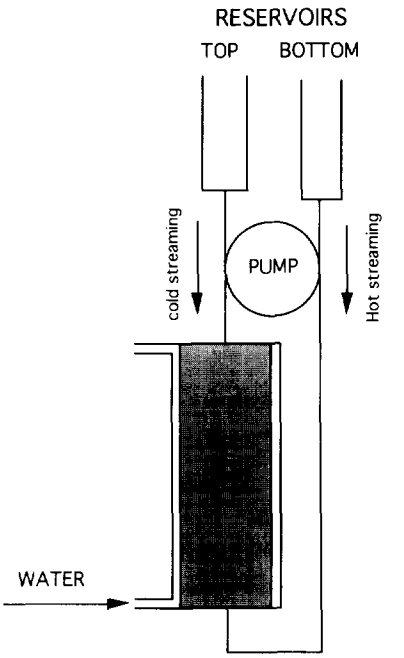

Fig. 2. Schematic diagram of parametric pumping.

Three parametric pumping runs were carried out under the conditions shown in Table 3. In addition to the amino acids at the given concentrations, the solution contains also in all runs an initial concentration of 1.0 *M* HCl. The experimental results are shown in Figs. 3–5. In Fig. 3 the experimental results obtained for threonine are not plotted because its initial concentration was less than that of the others (see Table 3, run 1) and the data would be confusing.

According to the temperature dependence of distribution coefficients for amino acids (Table 2), the concentration of each amino acid decreases in the bottom reservoir and increases in the top reservoir. With increasing number of cycles, the increase in amino acid concentrations in the top reservoir becomes more and more slow and after a certain number of cycles it turns

Table 3
Experimental conditions

Run	Displaced volume (cm^3)	Amino acid	Initial concentration (mmol/l)	Column length (cm)
1	50	Asp	30	50
		Thr	12.5	
		Ser	30	
		Glu	30	
2	10	Asp	30	50
		Thr	30	
		Ser	30	
		Glu	30	
3	10	Asp	60	50
		Thr	60	
		Ser	60	
		Glu	60	

into a slight decrease (this is not very apparent on the figures, owing to the logarithmic scale). It seems that this phenomenon occurs when the number of cycles and the initial concentrations are large enough and the displaced volume is small, as in run 3. The higher amino acid concentrations lead to competition for the ion-exchange sites, and probably that is the reason why the threonine concentration increases only slowly in the top reservoir at the beginning of the experiment and decreases after eleven cycles (the top reservoir concentrations for run 3 are given in Table 4). The results demonstrate the capability of thermal parametric pumping for concentrating amino acids from acidic mixtures.

In addition, the results indicate the importance of the difference between the hot and cold equilibrium distributions (K_c/K_h). The initial concentration ratio in run 3 was 1:1:1:1, which changed to 4.85:1:1.97:5.39 after twenty cycles (aspartic acid, threonine, serine, glutamic acid, respectively). Hence one can conclude that the larger is K_c/K_h, the greater is the concentrating effect of amino acids.

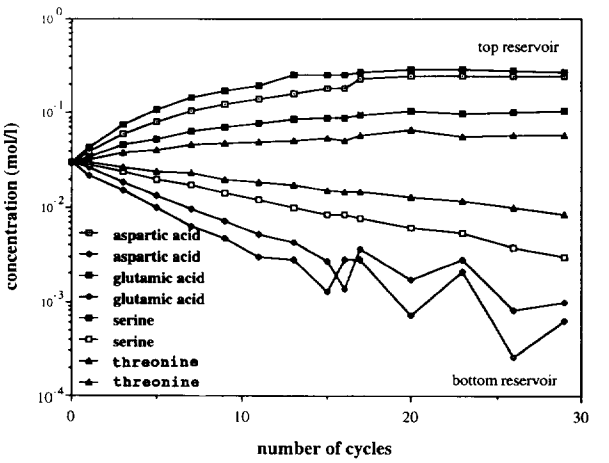

Fig. 4. Experimental results of amino acid parametric pumping (run 2).

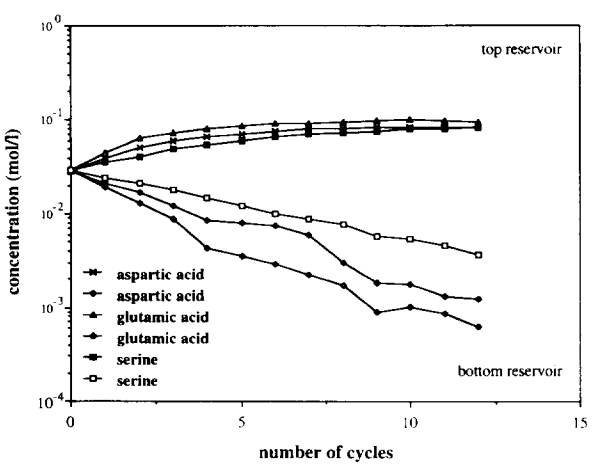

Fig. 3. Experimental results of amino acid parametric pumping (run 1).

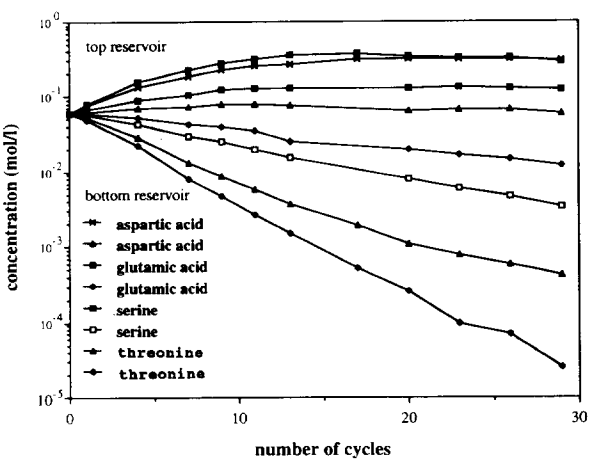

Fig. 5. Experimental results of amino acid parametric pumping (run 3).

Table 4
Top reservoir concentrations for run 3

Cycle No.	Asp	Thr	Ser	Glu
0	0.06	0.06	0.06	0.06
1	0.0752	0.0618	0.067	0.0803
4	0.1352	0.0691	0.0891	0.1617
7	0.1876	0.0727	0.1058	0.2316
9	0.2324	0.0781	0.1235	0.2869
11	0.2552	0.0791	0.1288	0.3151
13	0.2755	0.0763	0.1323	0.3589
17	0.3228	–	–	0.3694
20	0.3177	0.0654	0.1288	0.3526
23	0.3177	0.0673	0.1341	0.338
26	0.3126	0.0673	0.1323	0.3297
29	0.3076	0.06	0.127	0.2921

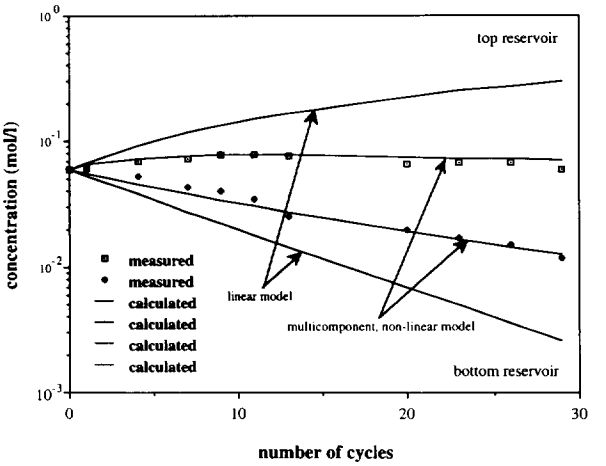

Fig. 7. Comparison of experimental and calculated results (run 3; threonine).

4.4. Comparison of experimental results with equilibrium parametric pumping models

The difference between the two models is that the first is a multi-component non-linear equilibrium model and the second is a linear equilibrium model (Pigford et al.'s model), which was developed first of all to understand the movement of the fronts and less to calculate the concentrations in the reservoirs. Typical results of calculations are shown in Figs. 6–10.

Both of the models seem to be sufficiently precise for run 1, that is, when the volume of displaced solution is 50 cm^3. In this case the amino acid concentrations in the cold reservoir are not so high, and the assumption of linear isotherms is close to reality.

The conditions are completely different if the volume of displaced solution is 10 cm^3. In this case the description with Pigford et al.'s model is

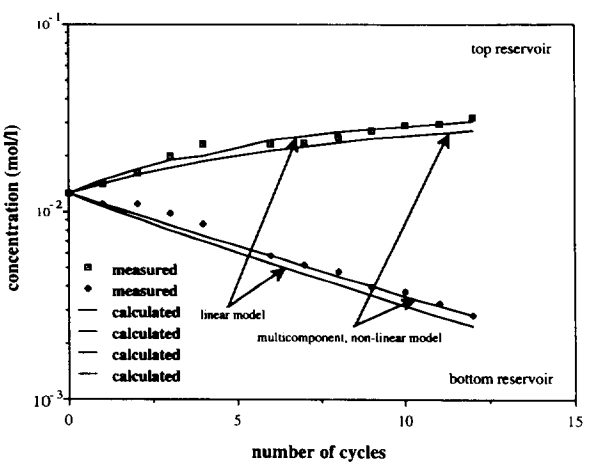

Fig. 6. Comparison of experimental and calculated results (run 1; threonine).

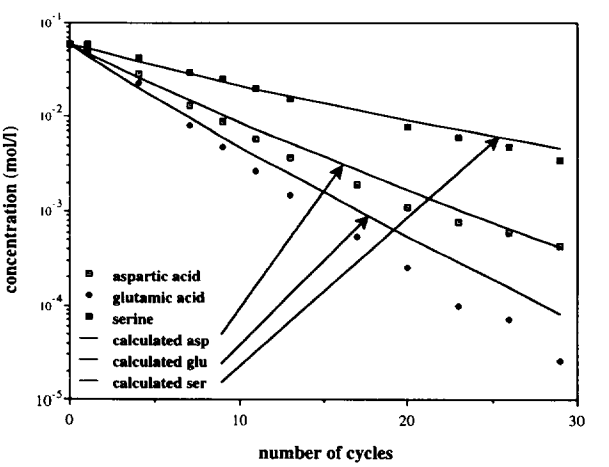

Fig. 8. Comparison of experimental and calculated results in bottom reservoir (run 3).

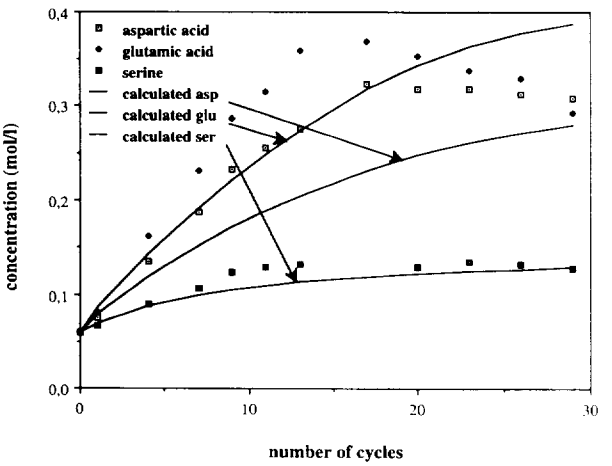

Fig. 9. Comparison of experimental and calculated results in top reservoir (run 3).

not sufficiently precise (Fig. 7). Since the volume of streamed solution is low, the concentrations in the top reservoir are much higher than in the previous case. As a result, the assumption of linear isotherms in Pigford et al.'s model is not true. Moreover, there is competition for the ion-exchange sites.

The multi-component model takes this competition into consideration by using the multi-component uptake of amino acids (Eq. 3) and the effect can be seen in Fig. 7. The great difference between the two models (Fig. 7) is caused by the competition for the resin sites. According to the equilibrium data and Eq. 3, the threonine uptake is less and decreases relative to the others, whereas the concentrations of the other amino acids increase. As the temperature dependence of its isotherm is lower, it is possible in such extreme conditions (after eleven cycles the concentrations of the other amino acids are much greater, see Table 4) that part of the column can take up more threonine at a hot than at a cold temperature. Maybe this is the reason why the threonine concentration begins to decrease in the top reservoir after eleven cycles (see Table 4). The multi-component model by applying Eq. 3 can calculate this concentration decrease in the top reservoir. The linear model considers the solution as a single-component solution, and hence it overestimates the separation.

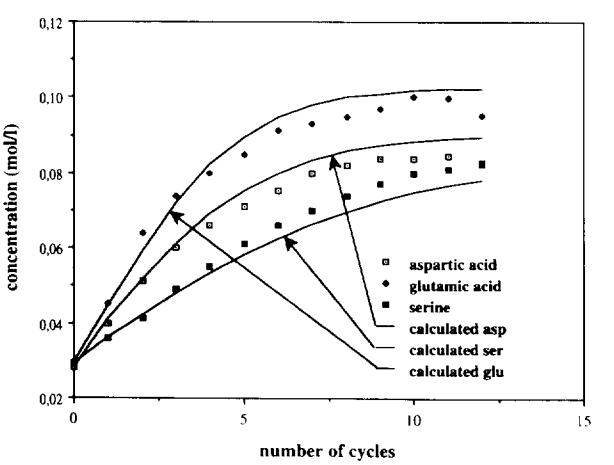

Fig. 10. Comparison of experimental and calculated results in top reservoir (run 1).

Figs. 8 and 9 show all the simulated (by the multi-component model) and experimental results of run 3, for the bottom and top reservoir, respectively. Fig. 8 shows good agreement of the calculated results with the experiments, except perhaps for glutamic acid. For this acid, the decrease in concentration is very significant (at $n = 29$, the concentration is $3 \cdot 10^{-5}$ mol/l, which is $5 \cdot 10^{-4}$ times the initial concentration) and a slight inaccuracy in the values of the distribution coefficients can explain this difference.

In Fig. 9, a linear concentration scale is used in order not to squash the curves. It can be seen that the simulations give the correct general behaviour of the experimental results. The simulation is good for serine. For aspartic and glutamic acid, the increase in experimental concentrations is faster than for the simulated ones, especially after about ten cycles, that is at rather high concentrations. This is probably due to the inaccurate description of the non-linear isotherms at relatively high concentrations. In fact, Eq. 3 assumes a constant selectivity coefficient, which is true for relatively low concentrations [17].

This interpretation is supported by the fact that good agreement is observed between experi-

ments and simulations when the concentrations are not so high, as in run 1, as shown in Fig. 10.

5. Theoretical study of the effect of chloride concentration

The experiments and simulations presented above apply to a given concentration of HCl (1 *M*). Because the hydrolysis can be performed at various acid concentrations, and also ion-exchange treatment of complex mixtures can remove a large amount of chloride, it is of interest to evaluate the behaviour of the separation as a function of the chloride content of the amino acid mixtures.

A mixture of only two amino acids, glutamic acid and proline, with various amounts of Cl^- (HCl) is considered. Glutamic acid was chosen because of the large variation of its distribution coefficient with temperature and proline because of its greater affinity for the resin relative to the other amino acids.

The complete multi-component non-linear model was used for this objective because the pH range considered is wide owing to the change of chloride concentration. If Eqs. 6–8 are inserted into Eq. 9 then C_{H^+} can be obtained numerically when values of C_{A_i} and C_{Cl^-} are assigned. If C_{H^+} is known, the ionic forms of amino acids can be calculated by Eqs. 5–8. These results are necessary for the calculation and we show some typical dissociation equilibria for glutamic acid and proline in Table 5 to facilitate the understanding of the theoretical treatment. At low pH the amino acids are protonated and predominantly in positively charged form, and the ionic fraction of hydrogen is high. When the solution pH is increased, amino acids become unprotonated and exist in zwitterionic or negatively charged form. It is also seen from Table 5 that on increasing the amino acid total concentrations in highly acidic solution both the proline and glutamic acid ionic fractions increase (first and last rows in Table 5), but on increasing the amino acid total concentrations in acid-free solution the proline ionic fraction decreases and the glutamic acid fraction increases (sixth and seventh rows in Table 5). The total amino acid concentrations in the last two rows are realistic results (the concentrations in the column solution are more or less those after

Table 5
Typical dissociation equilibria for glutamic acid and proline

C_{Cl} (mol/l)	Amino acid	Concentration (mol/l)					Amino acid ionic fraction
		Total amino acid	Cationic form	Anionic form	Zwitterionic form	Hydrogen (mol/l)	
1.0	Pro	0.05	$4.94 \cdot 10^{-2}$	$1.56 \cdot 10^{-14}$	$5.61 \cdot 10^{-4}$	0.9	0.0494
	Glu	0.05	$4.96 \cdot 10^{-2}$	$2.22 \cdot 10^{-8}$	$3.55 \cdot 10^{-4}$		0.0496
0.5	Pro	0.05	$4.87 \cdot 10^{-2}$	$7.75 \cdot 10^{-14}$	$1.24 \cdot 10^{-3}$	0.4	0.0978
	Glu	0.05	$4.92 \cdot 10^{-2}$	$1.1 \cdot 10^{-7}$	$7.9 \cdot 10^{-4}$		0.0988
0.1	Pro	0.05	$3.54 \cdot 10^{-2}$	$1.47 \cdot 10^{-11}$	$1.45 \cdot 10^{-2}$	0.025	0.354
	Glu	0.05	$3.96 \cdot 10^{-2}$	$2.32 \cdot 10^{-5}$	$1.03 \cdot 10^{-2}$		0.396
0.05	Pro	0.05	$1.91 \cdot 10^{-2}$	$1.21 \cdot 10^{-10}$	$3.08 \cdot 10^{-2}$	$6.3 \cdot 10^{-3}$	0.381
	Glu	0.05	$2.47 \cdot 10^{-2}$	$2.21 \cdot 10^{-4}$	$2.5 \cdot 10^{-2}$		0.493
0.01	Pro	0.05	$4.59 \cdot 10^{-3}$	$1.1 \cdot 10^{-10}$	$4.54 \cdot 10^{-2}$	10^{-3}	0.376
	Glu	0.05	$6.6 \cdot 10^{-3}$	$2.23 \cdot 10^{-3}$	$4.11 \cdot 10^{-2}$		0.541
0.0	Pro	0.05	$2.05 \cdot 10^{-3}$	$2.73 \cdot 10^{-9}$	$4.79 \cdot 10^{-2}$	$4.4 \cdot 10^{-4}$	0.384
	Glu	0.05	$2.84 \cdot 10^{-3}$	$5.34 \cdot 10^{-3}$	$4.18 \cdot 10^{-2}$		0.533
0.0	Pro	0.06	$2.57 \cdot 10^{-3}$	$3.14 \cdot 10^{-9}$	$5.74 \cdot 10^{-2}$	$4.58 \cdot 10^{-4}$	0.357
	Glu	0.07	$4.16 \cdot 10^{-3}$	$7.19 \cdot 10^{-3}$	$5.86 \cdot 10^{-2}$		0.578
1.0	Pro	0.06	$5.93 \cdot 10^{-2}$	$2 \cdot 10^{-14}$	$6.96 \cdot 10^{-4}$	0.87	0.0593
	Glu	0.07	$6.94 \cdot 10^{-2}$	$3.32 \cdot 10^{-8}$	$5.14 \cdot 10^{-4}$		0.0694

heating in the first cycle). Owing to the amphoteric character of amino acids, the HCl concentration has a great effect on the amino acid separation.

5.1. Saturation of the column

We calculated breakthrough curves for different concentrations of HCl in the saturation feed. In all instances, the initial form of the resin is H^+. The breakthrough volume is defined as the inflection point of the front. The solution pH of an amino acid in distilled water, when $C_{Cl} = 0$, approaches the isoelectric pH of the amino acid. For these conditions competition with hydrogen ions for the resin functional groups is at a minimum and the uptake reaches a maximum (see Eq. 3: if x_H is small, then y_{A_i} is large). As the chloride concentration is increased by adding HCl, the pH decreases, and the amino acid has to compete with hydrogen ions for the resin sites (see Eq. 3: if x_H is large, then y_{A_i} is small). The amount of amino acid taken up by the resin decreases for these conditions and therefore the breakthrough volume also. The breakthrough volume is higher for proline owing to the greater affinity of this amino acid for the resin.

Fig. 11 shows the dependence of amino acid breakthrough on chloride concentration.

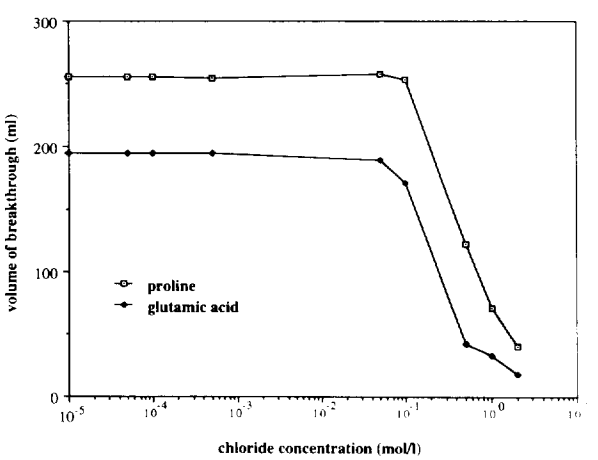

Fig. 11. Dependence of amino acid breakthrough on chloride concentration.

5.2. Results and discussion

At different displaced volumes the calculated separation factors (defined as concentration in the top reservoir/concentration in the bottom reservoir) of glutamic acid and proline, as a function of the chloride concentration, are indicated in Table 6 and in Figs. 12–14. One can see that the separation factor has a maximum and this value is in the high chloride concentration range.

The question arises of the reason for the important change in separation factors. Let us examine separately the highly acidic range and the acid-free (or acid-poor) range.

High chloride concentration range

When the chloride concentration is high the amino acids are positively charged (Table 5), and in this instance they behave like every cation. According to the temperature dependence of their distribution coefficients (Table 2),

Table 6
Separation factors of glutamic acid and proline

Amino acid	C_{Cl} (mol/l)	ΔV (cm^3)			
		5	10	20	100
Glu	0.0	28.50	4.59	2.52	1.86
Pro		11.40	1.45	0.64	0.56
Glu	0.00001	28.52	4.59	2.52	1.86
Pro		11.40	1.45	0.64	0.56
Glu	0.00005	28.58	4.59	2.52	1.86
Pro		11.39	1.45	0.64	0.56
Glu	0.0001	28.66	4.6	2.52	1.86
Pro		11.38	1.45	0.64	0.56
Glu	0.0005	29.12	4.61	2.53	1.87
Pro		11.28	1.45	0.64	0.56
Glu	0.05	15.51	9.61	3.93	1.81
Pro		6.70	3.0	0.99	0.60
Glu	0.1	18.36	18.37	11.30	1.25
Pro		6.20	4.84	2.59	0.82
Glu	0.5	453.37	791.85	256.61	1.11
Pro		25.87	78.38	141.43	3.45
Glu	1.0	1129.1	571.26	53.06	1.12
Pro		89.18	260.98	221.59	1.52
Glu	2.0	510.94	85.85	2.88	1.06
Pro		232.37	305.69	78.1	1.18

Initial concentration, 0.05 mol/l of each amino acid; volume of the resin, 10 cm^3; after 25 cycles.

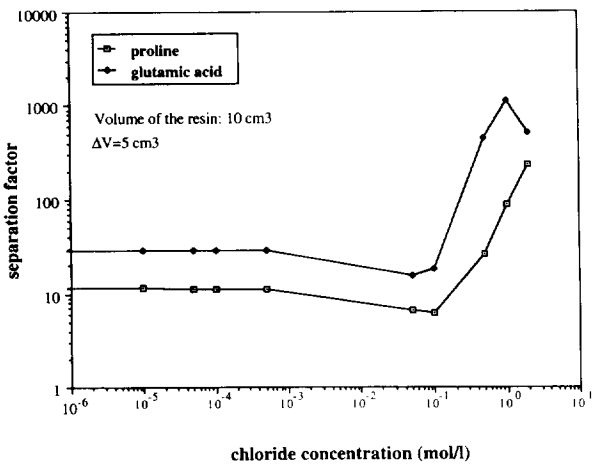

Fig. 12. Dependence of separation factor on chloride concentration (after 25 cycles).

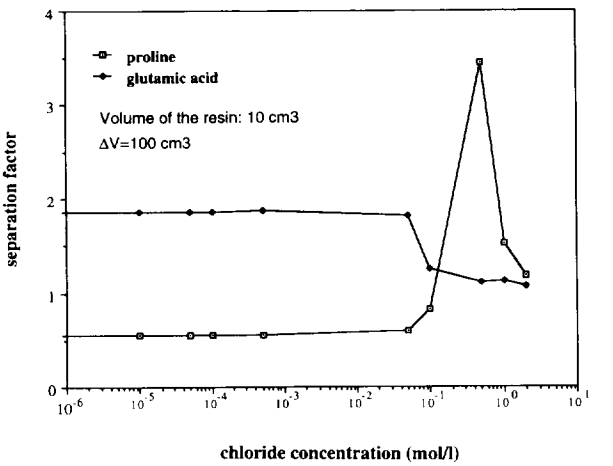

Fig. 14. Dependence of separation factor on chloride concentration (after 25 cycles).

the concentration of both amino acids decreases in the bottom reservoir and increases in the top reservoir (Fig. 1), and consequently their separation factor is greater than 1.

Further, one can observe that on increasing the chloride concentration the separation factor first increases and then decreases, and the position of the maximum value shifts from $C_{Cl} = 1$ to 0.5 mol/l on increasing the volume of displaced solution (except when $\Delta V = 100$ cm^3).

At the highest chloride concentration ($C_{Cl} = 2$ mol/l) the separation factor of glutamic acid is always less than at $C_{Cl} = 1$ mol/l and decreases on increasing the volume of the solution pumped through the column (Table 5). The competition for the resin functional groups is so unequal that the resin sites are mainly occupied by H^+ (Eq. 3) and therefore glutamic acid is "pushed" into the bottom reservoir, thereby spoiling the separation.

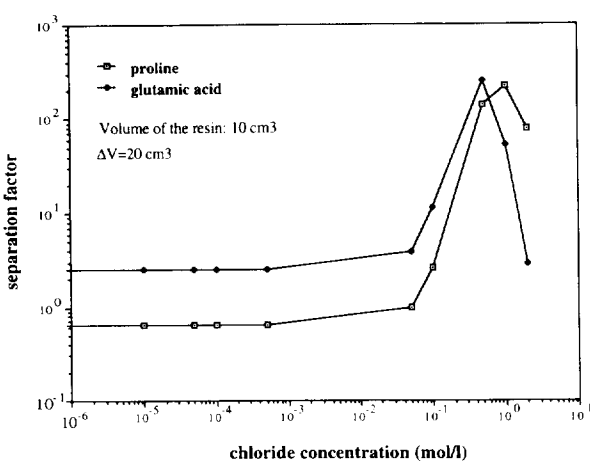

Fig. 13. Dependence of separation factor on chloride concentration (after 25 cycles).

Owing to the greater selectivity of proline, the decrease in its separation factor is slower. That is the reason why the proline separation factor becomes greater than that of glutamic acid as the streamed volume increases [in spite of the fact that the difference between hot and cold equilibrium distributions (K_c/K_h) is less for proline than glutamic acid].

The results of calculation for chloride concentrations from 2 to 0.5 mol/l show a maximum separation factor of glutamic acid (except when $\Delta V = 100$ cm^3), and this maximum value changes with the volume of displaced solution. On increasing ΔV, the maximum glutamic acid separation factor first decreases slowly and then rapidly, and the position of the maximum shifts towards lower chloride concentrations. The reasons for the shift are also the "competition" and the "push" of glutamic acid into the reservoir. If the competition for the ion-exchange

sites is intensive and the streamed volume is large (see Fig. 13; where $\Delta V = 20$ cm^3, $C_{Cl} = 1.0$ mol/l), glutamic acid is "pushed" out of the column and its separation factor is lower. If the intensity of the competition is less (see Fig. 13; where $\Delta V = 20$ cm^3, $C_{Cl} = 0.5$ mol/l) glutamic acid is not "pushed" out (or less), and the separation becomes better. A similar effect is observed for proline.

In Fig. 14, the displaced volume is so high that the separation factor for glutamic acid is very low. There is virtually no fixation of glutamic acid on the resin and thus no parametric pumping. For proline, which has a greater affinity, a parametric pumping effect can be seen but its separation factor is also small, because of the high streamed volume.

Low chloride concentration range

In this range, one can observe three characteristic features: first, the separation factors are low, second, they are almost constant, and, third, the glutamic acid separation is always higher than that of the proline.

In fact, in this low acidity range, the phenomena are completely different from those in the highly acidic range. Here there are only a few H^+ ions (see Table 5) so all the resin sites are occupied by amino acids (according to Eq. 3). Also, the amino acids are predominantly in the zwitterionic form. As the column is in the amino acid form and there is only a small difference between the amino acid ionic fractions in the reservoir and in the column solution (see the sixth and seventh rows of Table 5), there is only a little ion exchange. Consequently, most of the zwitterionic forms travel in the column without being fixed and thus do not participate in the parametric pumping. This is the explanation of why the separation factors are so low. They are constant because the amount of H^+ does not change very much until $C_{Cl^-} = 0.1$ mol/l, that is the total concentration of the two amino acids.

Finally, the separation factors decrease on increasing ΔV, as usual. However, for proline, the separation factor can be lower than 1 (Fig. 13), leading to a separation between glutamic acid and proline. This is explained below.

Separation of glutamic acid and proline

It can be seen in Figs. 12–14 that, in the low chloride concentration range, increasing ΔV leads to a decrease in the proline separation factor which shifts to values lower than unity. This is not the case for glutamic acid. Thus, the proline concentration increases in the bottom reservoir and that of glutamic acid in the top reservoir (Fig. 15). These two amino acids are thus separated. This contrasts with what could be expected from the temperature dependence of equilibrium distributions. The explanation is as follows.

After the column has become equilibrated, the same solution is contained in the column and in the bottom reservoir. When the column is heated the amino acid concentrations increase in the solution which is in the column, and as the temperature dependence of the glutamic acid equilibrium distribution is greater than that for the proline, the glutamic acid concentration in the column is higher than the proline concentration. As a result, the ionic fraction of glutamic acid is greater than in the bottom reservoir solution, and the ionic fraction of proline in the column solution is less than in the bottom reservoir solution (see the sixth and seventh rows of Table 5). [This is the essential difference between parametric pumping in highly acidic

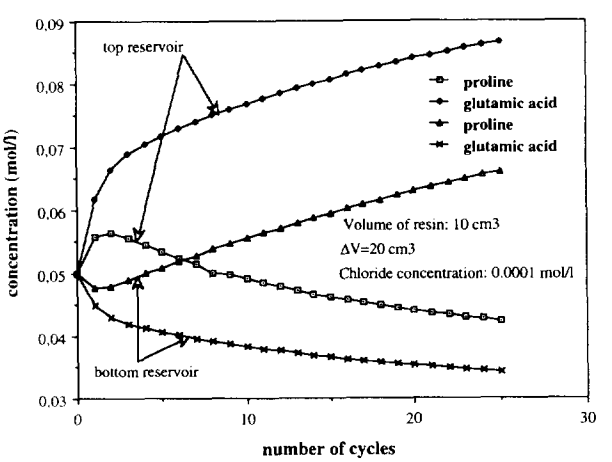

Fig. 15. Calculated results of amino acid parametric pumping.

solution and parametric pumping in acid-free solution. In highly acidic solution both the glutamic acid and proline ionic fractions in column solution are greater than in the bottom reservoir solution (see the first and last rows of Table 5).] As the resin is in equilibrium with a solution in which the proline ionic fraction is less than in the bottom reservoir, when the solution is pumped from the bottom to the top reservoir the column is able to take up proline. Consequently, the solution reaching the top reservoir first is rich in proline, because of the desorbed proline, and subsequently contains less and less proline, and if ΔV is large enough the mixed concentration becomes less than the initial concentration.

When the column is cooled, the amino acid is taken up by the resin and as the temperature dependence of the glutamic acid equilibrium distribution is greater than that for proline, relatively more glutamic acid than proline is taken up. The glutamic acid ionic fraction becomes lower in the column solution than in the top reservoir solution, so when we begin to stream from the top towards the bottom reservoir, glutamic acid becomes a more favourable component. If ΔV is large enough it can exclude some proline out of the column to the bottom reservoir, and the proline concentration begins to increase in the bottom reservoir.

6. Conclusions

The separation of amino acids by thermal parametric pumping was investigated experimentally and theoretically. A multi-component, non-linear model that takes into account the dissociation reaction in the liquid phase was mainly used to predict the separation. Comparing the experimental with the calculated results, one can see that they are in good agreement, and the differences are probably caused by the inaccurate description of the hot or cold isotherms (or both) in the higher concentration range.

The experiments were carried out in a highly acidic solution, but it can be also very interesting to study the separation in a solution with low HCl content, because usually the complex amino acid mixtures are treated by ion exchange, which removes a large amount of chloride. Therefore, the model mentioned before was also used to study theoretically the effect of chloride concentration on the separation.

In the highly acidic range the amino acids behave like every cation and are not able to dissociate, and therefore according to the temperature dependence of the equilibrium distributions their concentrations increase in the top and decrease in the bottom reservoir. In this way the amino acids can be concentrated to different extents.

In acid-free conditions most of the amino acids are in the zwitterionic form and travel in the column mostly without participating in the parametric pumping, which is the reason for the low separation factor. Owing to the effect of the dissociation reaction in the liquid phase, amino acid separation can be observed (the glutamic acid concentration increases in the top reservoir and the proline concentration increases in the bottom reservoir), which is in contrast with the result expected from the temperature dependence of the distribution coefficient.

These results show that parametric pumping is capable of both concentrating and separating amino acids and the results depend strongly on the chloride concentration.

List of symbols

A	cross-sectional area of column (cm^2)
C	liquid-phase concentration (mol/l)
C_{A_i}	liquid-phase amino acid concentration (mol/l)
$C_{A_i^+}$	liquid-phase amino acid cation concentration (mol/l)
$C_{A_i^-}$	liquid-phase amino acid anion concentration (mol/l)
$C_{A_i^{2-}}$	liquid-phase amino acid anion concentration (mol/l)
$C_{A_i^\pm}$	liquid-phase zwitterionic amino acid concentration (mol/l)
C_c	liquid-phase concentration at cold temperature
C_{Cl}	chloride concentration (mol/l)

C_{H^+} liquid-phase hydrogen concentration (mol/l)
C_h liquid-phase concentration at hot temperature
C_n concentration in the bottom reservoir after n cycles
C_0 initial concentration (mol/l)
K_{1i} first dissociation equilibrium constant (mol/l)
K_{2i} second dissociation equilibrium constant (mol/l)
K_{3i} third dissociation equilibrium constant (mol/l)
K_c distribution coefficient at 288 K
K_h distribution coefficient at 363 K
K^T distribution coefficient at temperature T
K_W ionic product of water (mol^2/l^2)
q_{A_i} resin amino acid concentration (mol/l dry resin)
q_c concentration in resin at cold temperature
q_h concentration in resin at hot temperature
q_0 resin ion-exchange capacity (mol/l dry resin)
R universal gas constant (J/mol · K)
S_i binary ion-exchange selectivity for cation i relative to hydrogen ion
$S^T_{i,j}$ selectivity coefficient for exchange of ion i with ion j at temperature T
T temperature (K)
t time (s)
u concentration velocity (cm/s)
u_c concentration velocity at cold temperature (cm/s)
u_h concentration velocity at hot temperature (cm/s)
v interstitial velocity (cm/s)
x_{A_i} liquid-phase ionic fraction of amino acid cation i
x_i^T liquid-phase ionic fraction of cation i at temperature T
x_H liquid-phase ionic fraction of hydrogen
y_{A_i} resin-phase ionic fraction of amino acid cation i
y_i^T resin-phase ionic fraction of cation i at temperature T
V_c volume of the bed (cm^3)
V_i volume of pulse injection (cm^3)
V_R retention volume of the amino acid (cm^3)
z bed axial position (cm)

Greek letters

ε bed void fraction
ΔH heat of ion-exchange reaction (J/mol)
ΔV volume of displaced solution (cm^3)

Acknowledgements

The experimental work was carried out at the University of Veszprem, Veszprem, Hungary, and the computer calculations were performed at Laboratoire des Sciences du Genie Chimique, Nancy, France. The financial support of the Hungarian Foundation "Peregrinatio I" is gratefully acknowledged.

References

[1] G. Grevillot and D. Tondeur, *AIChE J.*, 22 (1976) 1055.
[2] G. Grevillot and D. Tondeur, *AIChE J.*, 23 (1977) 840.
[3] R.H. Wilhelm, A.W. Rice and A.R. Bendelius, *Ind. Eng. Chem. Fundam.*, 5 (1966) 141.
[4] R.H. Wilhelm and N.H. Sweed, *Science*, 159 (1968) 522.
[5] R.L. Pigford, B. Baker and D.E. Blum, *Ind. Eng. Chem. Fundam.*, 8 (1969) 144.
[6] R. Aris, *Ind. Eng. Chem. Fundam.*, 8 (1969) 603.
[7] H.T. Chen and F.B. Hill, *Sep. Sci.*, 6 (1971) 411.
[8] H.T. Chen, J.L. Rak, J.D. Stokes and F.B. Hill, *AIChE J.*, 18 (1972) 356.
[9] H.T. Chen, E.H. Reiss, J.D. Stokes and F.D. Hill, *AIChE J.*, 19 (1973) 589.
[10] J.E. Sabadell and N.H. Sweed, *Sep. Sci.*, 5 (1970) 171.
[11] R. Rice, *Sep. Purif. Methods*, 5 (1976) 139.
[12] P.C. Wankat, *Sep. Sci.*, 9 (1976) 85.
[13] H.T. Chen, in P.A. Schweitzer (Editor), *Handbook of Separation Techniques for Chemical Engineers*, McGraw-Hill, New York, 1979, Sect. 1.15, p. 467.
[14] G. Grevillot, in N.P. Cheremisinoff (Editor), *Handbook of Heat and Mass Transfer*, Vol. 2, Gulf, Houston, 1986, Ch. 36.
[15] G. Carta, M.S. Saunders, J.P. DeCarli, II, and J.B. Vierow, *AIChE Symp. Ser.* 84 (1988) 54.
[16] M.S. Saunders, J.B. Vierow and G. Carta, *AIChE J.*, 35 (1989) 53.
[17] S.R. Dye, J.P. DeCarli, II, and G. Carta, *Ind. Eng. Chem. Res.*, 29 (1990) 849.
[18] L. Hanak, T. Szanya and G. Simon, in M. Perrut (Editor), *Proceedings of the 9th International Symposium on Preparative and Industrial Chromatography, Nancy*, INPL, Nancy, 1992, p. 185.